Vietnam Journal of Catalysis and Adsorption
Tạp chí xúc tác và hấp phụ Việt Nam

https://jca.edu.vn

Synthesis, photophysical characterization, aggregation-induced emission effect and crystal structure of (*E*)-butyl-3,3'-(5,6-dicarbazolylbenzo[c][1,2,5]thiadiazolyl)acrylate

Nguyen Van Gioi[1], Mai T. Phung[1], Phuong T. M. Ngo[1], Trang T. T. Pham[1], Duc H. Ta[1], Quang T. Tran[1], Ly P. Giang[1,*], Tung T. Dang[1,*]

[1] *School of Chemistry and Life Science, Hanoi University of Science and Technology, 1 Dai Co Viet Road, Hanoi, VIETNAM*
** Email: tung.dangthanh@hust.edu.vn; ly.giangthiphuong@hust.edu.vn*

Collection on 2025 International Symposium on Sustainable Catalysis (ISSC 2025-PRE APCAT 10)

ARTICLE INFO

Received: 29/09/2025
Accepted: 06/12/2025
Published: 30/12/2025

Keywords:
BINOL; BINAM;
Carbazole;
Benzo[2,1,3]thiadiazole;
Nucleophilic Substitution;
SnAr

ABSTRACT

In this study, we report the development of a simple and highly efficient synthetic protocol for the preparation of novel (E)-butyl-3,3'-(5,6-dicarbazolylbenzo[c][1,2,5]thiadiazolyl)acrylate via Heck cross-coupling reactions catalyzed by palladium. Optimized conditions utilizing a $Pd(OAc)_2/K_2CO_3$ system afforded high yields (70%), resulting in the successful synthesis and characterization (^{1}H-NMR, ^{13}C-NMR) of a new compound. Detailed investigations into its photophysical properties revealed pronounced aggregation-induced emission (AIE) behavior. Single-crystal X-ray diffraction analysis provided insights into the molecular packing and structure–property relationships, while computational chemistry supported the understanding of its electronic features. This work presents a valuable contribution to the field of C–C cross-coupling chemistry, offering a practical and versatile approach for the synthesis of diverse 4,7-dialkylated-5,6-N,N-dicarbazolylbenzothiadiazole derivatives, with potential applications in medicinal chemistry and materials science.

Introduction

Red and near-infrared (NIR) emission, typically spanning 620–900 nm, is of paramount importance in biomedical imaging owing to its superior tissue penetration, reduced light scattering, and minimal interference from endogenous autofluorescence [1] [2]. These optical windows facilitate high-resolution, non-invasive imaging, thereby enabling precise visualization of biological structures in vivo. Moreover, the advancement of NIR-emitting materials has significantly broadened their applicability across fields such as photodynamic therapy, bioimaging probes, and organic optoelectronic devices [3].

The 2,1,3-benzothiadiazole (BTD) scaffold has emerged as a pivotal building block in the design of advanced π-conjugated systems due to its strong electron-withdrawing nature, high thermal and photochemical stability, and intrinsic planarity [4] [5]. As a versatile and synthetically accessible heterocycle, BTD enables fine-tuning of electronic structures via donor–acceptor (D–A) engineering, making it highly suitable for a range of optoelectronic applications including organic light-emitting diodes (OLEDs), field-effect transistors, and photovoltaic devices [6]. Its quinoid-like resonance form contributes to enhanced charge transfer characteristics, while its modularity allows for straightforward functionalization at the 4,7-positions through cross-

https://doi.org/10.62239/jca.2025.054

coupling techniques such as Suzuki, Heck, and Sonogashira reactions [7]. In recent years, BTD-based small molecules and polymers have gained prominence not only for their role as electron-accepting motifs in semiconducting materials but also for their emerging utility in biological imaging and sensing, owing to their large Stokes shifts, bright emission, and cellular permeability [4, 7].

Carbazole and its derivatives have emerged as privileged electron-donating units in the design of conjugated materials due to their rigid planar structures, high hole-transport ability, and favorable thermal and oxidative stability[8, 9]. The electron-rich nature of the carbazole core facilitates effective intramolecular charge transfer (ICT) when coupled with electron-accepting moieties, contributing to bathochromic shifts and enhanced photoluminescence in donor–acceptor (D–A) architectures [10]. Owing to its modifiable positions, particularly at the 3-, 6-, and 9-sites, carbazole allows for synthetic versatility through cross-coupling and electrophilic substitution strategies, enabling fine-tuning of electronic and photophysical properties [11]. Incorporation of carbazole into fluorescent frameworks has also demonstrated remarkable aggregation-induced emission (AIE) or enhanced emission (AIEE) behaviors by restricting intramolecular motion and suppressing π–π stacking in the aggregated state. These features, combined with excellent biocompatibility and two-photon absorption potential, have broadened the application of carbazole-based systems beyond optoelectronics to include targeted bioimaging, molecular sensing, and theranostics [8, 9].

Benzothiadiazole (BT, or 2,1,3-benzothiadiazole) is a highly electron-deficient heteroaromatic unit that has become a key building block in organic electronics. It plays a strong role in sensing applications and in organic field-effect transistors (OFETs) due to its electron-accepting ability, planarity, and ability to tune optoelectronic properties. Here's a structured breakdown of how it functions: ion sensing (metal cations, anions), pH and proton sensing, advantages in sensing bue to high quantum yield, strong signal change uppon interaction, tunable emission (blue to nir) and good chemical stability. Benzothiadiazole acts as a strong electron acceptor and optical reporter. In sensing, its donor–acceptor interactions enable sensitive detection of ions, protons, and environmental changes via fluorescence modulation. In OFETs, BT stabilizes electron transport, tunes energy levels, and promotes ambipolar behavior, making it crucial for high-performance organic semiconductors. Light-responsive BT-based OFETs can be used for photodetectors, logic circuits, and memory devices. Key Advantages of BT in OFET-based devices and promising for glucose sensing because of strong electron-accepting unit, optical reponsiveness, donor-acceptor tunnability and possible thin-film spincoating.

H. Shi *et al.* (2019) have successfully synthesized a benzothiadiazole derivative bearing two rigid carbazole units (DBCz-BT) that exhibits efficient red phosphorescence with enhanced triplet stability and suppressed nonradiative decay [12]. In view of the potential of red phosphorescence in biomedical applications, we further functionalized the compound (DBCz-BT) with a single step Heck cross-coupling reaction. The two bromine in the position of the compound (DBCz-BT) are possible to tunnable the absorption, emission and solubility in fabrication of non-invasive blood glucose monitoring devices.

Experimental

Starting reagents were purchased commercially and used without further purification, except for 4,7-dibromo-5,6-N,N-dicarbazoyl benzothiadiazole (DBCz-BT), which was synthesized and modified according to the literature methods of H. Shi *et al.* (2019).

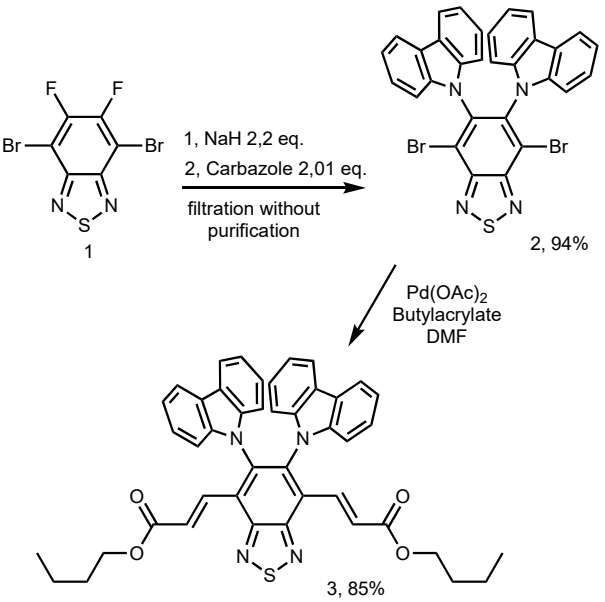

Scheme 1: Synthesis of (E)-butyl-3,3'-(5,6-dicarbazolylbenzo[c][1,2,5]thiadiazolyl)acrylate

Measurement. ^{1}H NMR spectra were recorded on a BRUKER 500 MHz Ascend spectrometer with tetramethylsilane (TMS) as the internal standard. UV–visible absorption spectra were obtained using Aligent Cary 5000. Steady-state fluorescence spectra and excitation spectra were measured using NanoLog

https://doi.org/10.62239/jca.2025.054

Horiba. X-ray single-crystal analysis was achieved by using a Rigaku XtaLabPro diffractometer equipped with a microfocus Mo K_α radiation and a HPAD PILATUS3 R 200K detector. CrysAlisPro was used for data processing, applying an empirical absorption correction using spherical harmonics, combined with a numerical approach, as implemented in the SCALE3 ABSPACK scaling algorithm.

Synthesis of 4,7 – dibromo – 5,6 – N,N –Dicarbazoyl-benzothiadiazole. Dry N,N-dimethylformamide (DMF, 10 mL) was injected to a 25 mL pressure tube charged with 9H-carbazole (504.14 mg, 3.02 mmol) and sodium hydride (60%) (131.99 mg, 3.01 mmol) under nitrogen protection. The resulting mixture was stirred at room temperature for 4.5 h. Then, a solution of 4,7-dibromo-5,6-difluoro-2,1,3- benzothiadiazole (494.91 mg, 1.5 mmol) in dry DMF (8 mL) was slowly added into the flask and stirred for 12 h at 110 °C to obtain an orange precipitate. The product was collected by vacuum filtration and washed with dichloromethane three times. The orange lamellar crystals were collected (886.42 mg, 94.65%).

Synthesis of (E)-butyl-3,3'-(5,6-dicarbazolylbenzo-[c][1,2,5]thiadiazolyl)acrylate (BABTD). Dry N,N-dimethylformamide (DMF, 3 mL) was injected to a 10 mL pressure tube charged with DBCz-BT (43.7 mg, 0.07 mmol), n-butyl acrylate (0.04 mL, 0.28 mmol), Pd(OAc)2 (1.57 mg, 0.007 mmol) and potassium carbonate (0.26 g, 4.5 mmol) under argon protection. The resulting mixture was stirred at 100 °C for 24 h. The reaction mixture was collected and extracted with dichloromethane/distilled water three times. The solvent was then removed by rotary vacuum. The product was purified by silica gel column chromatography, and its structures were verified by ^{1}H-NMR, ^{13}C-NMR.

^{1}H-NMR (500 MHz, $CDCl_3$): δ (ppm) 7.90 (d, J = 16.1 Hz, 1H), δ 7.65 (d, J = 7.7 Hz, 2H), δ 7.37 (d, J = 16.1 Hz, 1H), δ 7.01 (m, J = 3.9 Hz, 2H), δ 6.92 (m, J = 4.1 Hz, 2H), δ 6.80 (d, J = 8.2 Hz, 2H), δ 4.01 (d, J = 6.5 Hz, 2H), δ 1.45 (m, J = 5.6 Hz, 2H), δ 1.12 (q, J = 7.5 Hz, 2H), δ 0.79 (d, J = 7.4 Hz, 3H).

^{13}C-NMR (126 MHz, $CDCl_3$): δ (ppm) 166.44, 153.05, 140.23, 137.62, 135.18, 128.93, 128.90, 125.00, 123.6, 120.4, 119.70, 110.34, 64.52, 30.43, 18.93, 13.64

Results and discussion

The molecule BABTD was synthesized by a one-step Heck cross-coupling reaction (Scheme 1), whose chemical structure was fully characterized by NMR and single-crystal analysis.

The compound demonstrates good solubility in common organic solvents such as chloroform ($CHCl_3$), tetrahydrofuran (THF), dichloromethane (DCM), and toluene, attributed to its branched molecular architecture. The absorption and emission spectra of BABTD were measured in dilute dichloromethane (DCM) solution, with the absorption spectrum presented in Figure 1. In solution, BABTD exhibits two prominent absorption bands centered at 477 nm and 379 nm, corresponding to the π–π* transition of the conjugated backbone (band I) and the intramolecular charge transfer (ICT) between donor and acceptor units (band II), respectively. These features indicate that BABTD functions as a typical donor–acceptor (D–A) system.

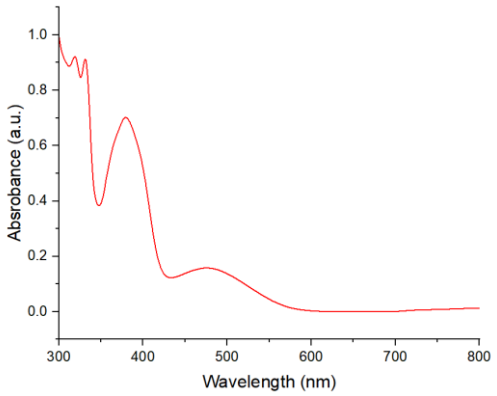

Fig. 1: Absorption spectra of BABTD

Notably, BABTD also displays an aggregation-induced emission (AIE) effect, demonstrating its potential in biomedical fields. Upon aggregation, BABTD exhibits a maximum emission (λ_{max}) at 623 nm, which corresponds to a red color, accompanied by a significant increase in emission intensity. This emission peak is red-shifted by 21 nm relative to that of DBCz-BT, attributable to the incorporation of a stronger electron-donating group. The molecule exhibited a pronounced Stokes shift of 146 nm, which is highly advantageous for practical applications. The unusually large Stokes shift minimizes spectral overlap between absorption and emission processes, reducing the likelihood of reabsorption losses in condensed phases. This is highly advantageous for applications requiring high photoluminescence quantum yields in dense films or biological imaging media.

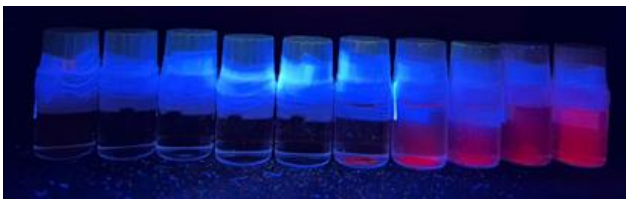

Fig. 2: Photos of BABTD in THF–water mixtures with different water fractions (left to right: 0–90%) under UV light illumination.

https://doi.org/10.62239/jca.2025.054

To gain deeper insight into the AIE effect, the emission spectra of BABTD was recorded in THF and THF–water mixtures with varying water fractions (f_w), enabling the investigation of their emission behavior as a function of aggregation. The AIE behavior was clearly observed as the water fraction increased. Weak or negligible emission was detected in pure THF, but upon increasing the water content to 70%, a distinct luminescence emerged, indicating the onset of aggregation-induced restriction of intramolecular motions. Further increasing the water fraction to 90% led to a significant enhancement in emission intensity, confirming the typical AIE characteristic. The progressive enhancement of fluorescence intensity upon increasing water fraction clearly reflects the aggregation-induced restriction of intramolecular rotations (RIR), which effectively channels the excited-state energy into radiative decay pathways. This observation confirms that molecular packing plays a pivotal role in suppressing nonradiative transitions.

The molecular packing and interactions were analyzed by the X-ray single-crystal study. In a single molecule, it showed a nonplanar molecular structure with multiple intramolecular interactions, including C–H···N (2.271, 2.306 Å), C–H···π (2.412, 2.582 Å), C–H···O (2.319, 2.353 Å), C···N (3.1 Å). Each core molecule was surrounded by four neighboring molecules through multiple C–H···O intermolecular interactions, which effectively restricted molecular motions and thereby suppressed nonradiative decay. The absence of strong π–π interactions, combined with multiple weak C–H···O contacts, suggests a packing arrangement that favors isolated emissive units, thereby reducing exciton quenching pathways. Such a packing mode is particularly advantageous for achieving high solid-state luminescence, an essential requirement for practical optoelectronic device applications.

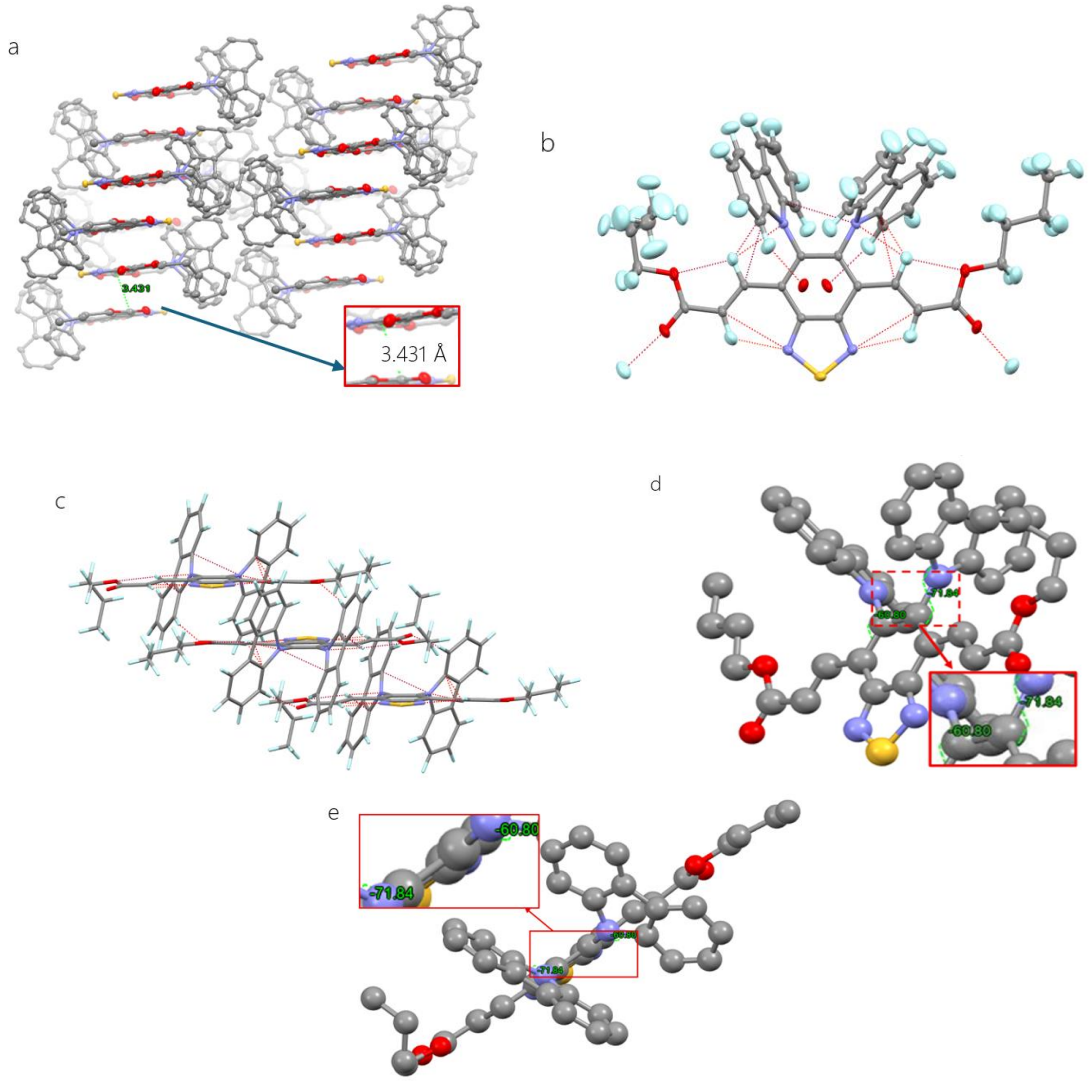

Fig. 3: X-ray crystal structure and investigation:(a) Packing diagram, (b-c) inter- and intramolecular distances, and (d-e) Solid-state structures of BABTD

https://doi.org/10.62239/jca.2025.054

The molecule exhibits a deep HOMO energy level of –5.95 eV and a LUMO level of –3.59 eV, resulting in a moderate energy gap of 2.36 eV. This electronic structure not only confers high oxidative stability and favorable energy alignment for charge injection but also supports efficient radiative decay pathways. The combination of a large Stokes shift and moderate bandgap indicates a strong intramolecular charge transfer character, which is beneficial for suppressing aggregation-caused quenching and promoting aggregation-induced emission behavior. These properties collectively highlight the material's promising potential for solid-state optoelectronic devices and bioimaging applications.

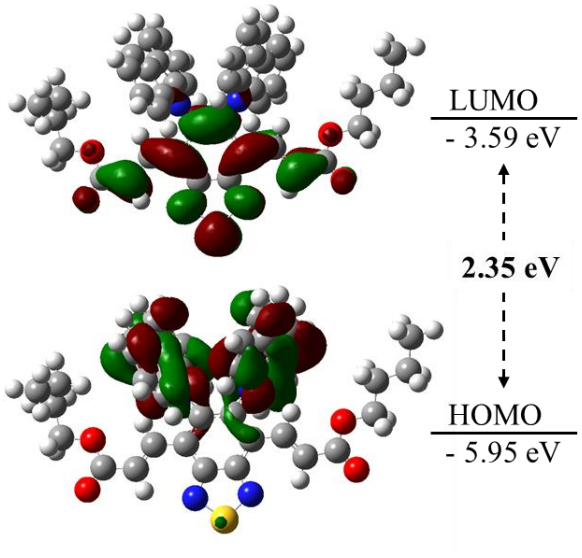

Fig. 4: HOMO-LUMO level of BABTD

Conclusion

In summary, we have developed a scalable and versatile synthetic approach to benzothiadiazole-based donor–acceptor systems with finely tuned electronic structures and strong aggregation-induced emission behavior. Structural rigidification via intramolecular C–H···O interactions and controlled crystal packing effectively restricted molecular motions, suppressing nonradiative decay. The deep HOMO levels and modulated LUMO energies underscore the potential of these materials for advancing solid-state luminescent and optoelectronic applications. The synthesis and photophyscial studies and also Xray crystal are well defined. These properties collectively highlight the material's promising potential for optoelectronic devices.

Acknowledgments

This research is funded by the Ministry of Science and Technology "Research, design and manufacture of non-invasive blood glucose monitoring devices using near-infrared (NIR) optical sensors for diabetes management application", Vietnam under grant number ĐTĐL.CN-31/23.

References

1. M. Dai, Y.J. Yang, S. Sarkar, K.H. Ahn, Chem. Soc. Rev., 52(18) (2023) 6344–6358. https://doi.org/10.1039/D3CS00475A
2. J. Wang, F. Huo, Y. Yue, C. Yin, Luminescence, 35(8) (2020) 1156–1173. https://doi.org/10.1002/bio.3831
3. M. Xu, X. Li, S. Liu, L. Zhang, W. Xie, Mater. Chem. Front., 7(20) (2023) 4744–4767. https://doi.org/10.1039/D3QM00585B
4. B.A.D. Neto, J.R. Correa, J. Spencer, Chem. Eur. J., 28(4) (2022) e202103262. https://doi.org/10.1002/chem.202103262
5. N.S. Gudim, S.S. Melnikov, K.Y. Shuvaev, A.Y. Sosorev, I.C. Avetissov, P.A. Stuzhin, Molecules, 26(16) (2021) 4931. https://doi.org/10.3390/molecules26164931
6. M. Hancharova, K. Mazur, K. Halicka, D. Zając, J. Polym. Res., 29(10) (2022) 417. https://doi.org/10.1007/s10965-022-03266-1
7. B.A.D. Neto, P.H.P.R. Carvalho, J.R. Correa, Acc. Chem. Res., 48(6) (2015) 1560–1569. https://doi.org/10.1021/ar500468p
8. A. Afrin, C.A.S. Pothulapadu, Mater. Chem. Front., (2025) 1794–1820. https://doi.org/10.1039/D5QM00238A
9. J. Yin, Y. Ma, G. Li, M. Peng, W. Lin, Coord. Chem. Rev., 412 (2020) 213257. https://doi.org/10.1016/j.ccr.2020.213257
10. Gupta, P.E. Kesavan, Front. Chem., 7 (2019) 841. https://doi.org/10.3389/fchem.2019.00841
11. L. Kong, T. Zhang, K. Yang, S. Cui, X. Tan, J. Mater. Sci., 53(2) (2018) 921–936. https://doi.org/10.1007/s10853-017-1570-z
12. H. Shi, H. Ma, W. An, Z. Lv, S. Gu, S. Wang, H. Ma, W. Tian, ACS Appl. Mater. Interfaces, 11(20) (2019) 18103–18110. https://doi.org/10.1021/acsami.9b01615